AFRL-SN-RS-TR-2007-41
Final Technical Report
February 2007

CHIP-SCALE CONTROLLED STORAGE ALL-OPTICAL MEMORY

University of California

Sponsored by
Defense Advanced Research Projects Agency
DARPA Order No. V407/00

AIR FORCE RESEARCH LABORATORY
SENSORS DIRECTORATE
ROME RESEARCH SITE
ROME, NEW YORK

NOTICE AND SIGNATURE PAGE

AFRL-SN-RS-TR-2007-41 HAS BEEN REVIEWED AND IS APPROVED FOR PUBLICATION IN ACCORDANCE WITH ASSIGNED DISTRIBUTION STATEMENT.

FOR THE DIRECTOR:

/s/	/s/
RICHARD FEDORS Work Unit Manager	RICHARD SHAUGHNESSY Chief, Rome Operations Office Sensors Directorate

REPORT DOCUMENTATION PAGE

Form Approved
OMB No. 0704-0188

1. REPORT DATE *(DD-MM-YYYY)*	2. REPORT TYPE	3. DATES COVERED *(From - To)*
FEB 2007	Final	Jun 02 – Oct 06

4. TITLE AND SUBTITLE

CHIP-SCALE CONTROLLABLE STORAGE OPTICAL MEMORY (CSOM)

5a. CONTRACT NUMBER

5b. GRANT NUMBER
FA8750-02-2-0096

5c. PROGRAM ELEMENT NUMBER
63739E

6. AUTHOR(S)

Constance Chang-Hasnain and Shun Lien Chuang

5d. PROJECT NUMBER
N584

5e. TASK NUMBER
SN

5f. WORK UNIT NUMBER
01

7. PERFORMING ORGANIZATION NAME(S) AND ADDRESS(ES)

University of California
2150 Shattuck Ave.
Berkeley CA 94704-5940

8. PERFORMING ORGANIZATION REPORT NUMBER

9. SPONSORING/MONITORING AGENCY NAME(S) AND ADDRESS(ES)

Defense Advanced Research Projects Agency
3701 North Fairfax Dr.
Arlington VA 22203-1714

AFRL/SNDP
25 Electronic Pkwy
Rome NY 13441-4515

10. SPONSOR/MONITOR'S ACRONYM(S)

11. SPONSORING/MONITORING AGENCY REPORT NUMBER
AFRL-SN-RS-TR-2007-41

12. DISTRIBUTION AVAILABILITY STATEMENT
APPROVED FOR PUBLIC RELEASE; DISTRIBUTION UNLIMITED. PA# 07-058

13. SUPPLEMENTARY NOTES

14. ABSTRACT

Goal of the project was to demonstrate a semiconductor waveguide device suitable for use as an all-optical buffer with a slow down factor of 1000 at room temperature. Theoretical and experimental research was performed to show the feasibility of slow light in semiconductor quantum wells. Prototype GaAs quantum well devices were fabricated, and characterized at both cryogenic and ambient laboratory temperatures. Mechanisms such as coherent population oscillation (CPO) and electromagnetically induced transparency (EIT) were explored. The results included several of the first ever achieved experimental and theoretical results on slow light, including the demonstration of a factor of one million times reduced light speed in semiconductor quantum wells at low temperature, a reduction of approximately 600 at room temperature, and the first observation of EIT in semiconductor quantum wells. Wide-spread interest in the subject led to an international conference starting in 2006, and helped spur new research into all-optical buffers.

15. SUBJECT TERMS
Slow light, all-optical buffer, optical delay, fast light, group velocity, semiconductor quantum wells, coherent population oscillation, electromagnetically induced transparency

16. SECURITY CLASSIFICATION OF:			17. LIMITATION OF ABSTRACT	18. NUMBER OF PAGES	19a. NAME OF RESPONSIBLE PERSON
a. REPORT	b. ABSTRACT	c. THIS PAGE			Richard Fedors
U	U	U	UL	28	19b. TELEPHONE NUMBER (*Include area code*)

TABLE OF CONTENTS

LIST OF FIGURES

GLOSSARY

AM	amplitude modulation
CPO	coherent population oscillation
CW	continuous wave
DBP	delay-bandwidth product
EIT	electromagnetically induced transparency
FOM	figure of merit
FP	Fabry-Perot
FWHM	full width at half maximum
FWM	four-wave mixing
GHz	giga Hertz
HH	heavy hole
HWHM	half width at half maximum
KHZ	kilo Hertz
KK	Kramers-Kronig
LH	light hole
MBE	molecular beam epitaxy
MHz	mega Hertz
MZI	Mach-Zehnder interferometer
QD	quantum dot
QW	quantum well
RF	radio frequency
RT	room temperature
SOA	semiconductor optical amplifier
SQW	single quantum well
TE	transverse electric
TM	transverse magnetic
VCSEL	vertical cavity surface-emitting laser
WG	wave guide

Chip-Scale Controlled Storage All-Optical Memory

PI: Connie Chang-Hasnain, University of California, Berkeley,
cch@eecs.berkeley.edu

Co-PI: Shun-Lien Chuang, University of Illinois, Urbana Champaign

EXECUTIVE SUMMARY

The final goal of the project is to demonstrate a semiconductor waveguide device suitable for use as an all-optical buffer with at least a slow down factor of 1000 at room temperature. During the last four years, we performed theoretical and experimental research on how to achieve slow light in semiconductors. We explored coherent mechanisms including coherent population oscillation (CPO) and electromagnetically induced transparency (EIT). Our results were the first to show that slow light can be achieved in semiconductors. It also opened a door for new research in this area.

In section 1, we provide some motivation for the subject. In section 2, we summarize the results obtained using CPO and section 3, EIT. Section 4 discusses figures of merit for optical communications applications, which is followed by some concluding remarks. The supported personnel and publications in this program are listed in the Appendix.

Chip-Scale Controlled Storage All-Optical Memory

1. Introduction

Optoelectronic technology played a pivotal role in the unprecedented information revolution in the past two decades. One of the remaining grand challenges is the ability to store an optical signal in optical format. Being able to keep data in the optical domain during the routing process is of particular interest because it can greatly reduce the routing delay caused by complex protocols, introduce data transparency for secure communications, and reduce the power and size of electronic routers.

A controllable optical delay line can effectively function as an optical buffer, where the storage is proportional to the variability of the group velocity. Due to the delay time which is not tunable, a fixed fiber delay loop or waveguide resonator alone cannot serve the function of an optical buffer. On the other hand, if the group velocity of light is controllable, we can generate a variable time delay. The capacity of buffering is directly proportional to the variability of the light velocity. Such an approach has received wide interest recently [1,2]. To date, the largest delay-bandwidth product (DBP) reported is approximately 4, which is still far from the application needs, which are several orders of magnitude larger [1,2]. However, current results with a tunable DBP~1 can be potentially useful for making a buffer consisting of a fine-adjusted tunable delay with a fixed long delay line. In addition, there may be other applications which do not require a very large DBP, such as ultra-low $V\pi$ modulators, true-time delay elements in microwave photonics, ultra-compact and low-power nonlinear optical components, optical signal processing, and quantum information processing [1, 2].

The basic principle of slow light centers on the definition of signal velocity, which is the same as group velocity, valid for most signals we use for optical communications because the bandwidth of the signal (1-100 GHz) is very small compared to the carrier frequency (193 THz). The group velocity v_g is defined as

$$v_g = \frac{\partial \omega}{\partial k} = \frac{c - \omega \dfrac{\partial n(k,\omega)}{\partial k}}{n(k,\omega) + \omega \dfrac{\partial n(k,\omega)}{\partial \omega}}, \qquad (1)$$

where c is the speed of light in vacuum, n is the real part of the refractive index, and k is the waveguide propagation constant. The slowdown factor S is thus

$$S = \frac{c}{v_g} = \frac{n + \omega \dfrac{\partial n}{\partial \omega}}{1 - \dfrac{\omega}{c}\dfrac{\partial n}{\partial k}}, \qquad (2)$$

which is equal to the group index. From (2), the group velocity can be reduced by introducing a large and positive waveguide dispersion $\partial n/\partial k$ or/and material dispersion $\partial n/\partial \omega$. It is important

to note that tunability of the slowdown factor is very critical. This is the key differentiator from a physical delay line, such as a long piece of fiber.

The material dispersion can be achieved by various methods to create gain or absorption spectral change. The waveguide dispersion can be designed using gratings, periodic resonant cavities, or photonic crystals [3, 4]. It is also possible to include both material and waveguide dispersions in one device to enhance the slowdown effect [5]. In this program, our primary attention has focused on material dispersion engineering using semiconductor devices.

Recently, various mechanisms have been used to obtain a large material dispersion for achieving slow slight. These include electromagnetically induced transparency (EIT) [1, 6], coherent population oscillations (CPO) [7-11], four-wave mixing (FWM) [12-16], stimulated Brillouin scattering [17, 18], stimulated Raman scattering [19, 20], etc. Tunable delay using semiconductor devices attracts much attention because it offers the advantage of compactness, room temperature operation, and easy integration with existing optical communication systems.

Slow (or fast) light can be obtained by introducing a change in the absorption (or gain) spectra of semiconductor quantum wells (QWs) and quantum dots (QDs). EIT in semiconductor quantum dots has been proposed and demonstrated [1, 21, 23]. Furthermore, recent experiments have been successful using CPO or FWM in quantum-well and quantum-dot devices from low to room temperatures. For example, the absorption (or gain) spectra can be changed via CPO [8-11,24], depletion of the exciton absorption peak [25], or wave-mixing in a semiconductor waveguide absorber [26]. In addition, both slow and fast light at room temperature can arise from the change in a sharp gain spectra, e.g. using a gain Fabry-Perot (FP) resonator or an integrated DFB-phase-shifter filter [27-29], QD semiconductor optical amplifiers (SOAs) [30-33], and a narrow-band VCSEL-SOA [34]. Recently, slow and fast light via four-wave mixing (FWM) in SOAs has been proposed, analyzed, and demonstrated using a single-beam or two beam (pump and probe) experimental setup [12-16]. Using optical injection locking as a technique, the radio frequency (RF) phase of the microwave-modulated signal can be shifted or delayed up to 2π by the slave laser, which effectively acts like a slow or fast light medium [35].

There have also been significant discussions about figures of merit, and in particular, discussions about the limiting mechanisms for the various approaches [2, 36-39]. Here, we review recent results we obtained under the support of this DARPA program.

2. Slow Light Using Coherent Population Oscillation in Quantum Wells [8-11, 24]

In a two-level system, the optical absorption peak corresponds to a negative derivative $\partial n / \partial \omega$ and leads to fast light, which is also called anomalous absorption dispersion. In the presence of an intense optical pump beam with the photon energy near the transition energy of the two-level system, absorption saturation occurs due to depletion of the population in the lower energy state. If a weak signal beam with a frequency slightly detuned from that of the pump beam is present, as shown in Fig. 1(a), the population of the excited state will beat at a frequency determined by the pump-signal detuning. Significant population beating occurs when the population can closely follow the intensity profile due to the time-dependent interference between the optical fields of the pump and signal beams. Thus, a reduction of the absorption, which shows a coherent spectral hole characterized by the inverse radiative lifetime, will be present, as shown in Fig. 1(b). From

the Kramers-Kronig (KK) relation, an absorption dip leads to a variation of the refractive index spectrum with a positive slope in the same frequency range, yielding the slow light effect.

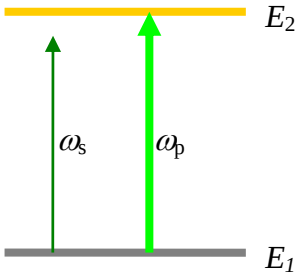

Fig. 1 (a) A two level system in the presence of a resonant pump and a detuned probe.

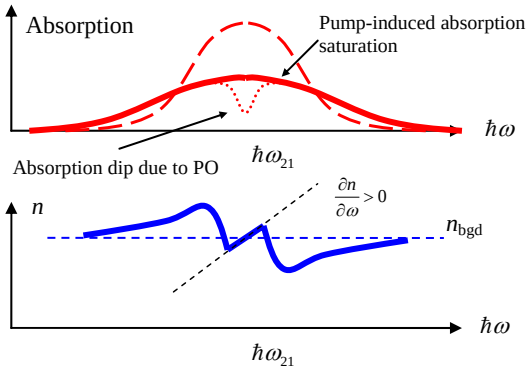

Fig. 1(b) Top- absorption spectrum of the probe in the absence (long dashed curve) and the presence (solid) of a strong pump. The spectral hole (dotted curve) is caused by CPO produced by the pump and probe beams. Bottom- the corresponding refractive index spectrum in the presence of CPO. [24]

To utilize the radiative lifetime, a pump-probe setup sensing CPO of the energy levels in the solid-state material system, such as ruby crystal, has been demonstrated [7] with bandwidth varying from 10 Hz up to kHz. In semiconductors, an example of such a quasi two-level system is the bound exciton state in QWs or self-assembled QDs. The nanosecond radiative lifetime in semiconductors corresponds to a gigahertz bandwidth and is suitable for practical applications. We describe CPO-based slow light from heavy-hole (HH) excitons in QWs [8-11]. We have also developed a theoretical model based on the density matrix formalism, taking into account the dipole selection rules and other nonlinear effects which couple the two spin subsystems [9]. Our theoretical results agree well with the experimental data [8].

2.1 Experimental Demonstrations

2.1.1 Measurements of Dispersion Curves

The following summarizes our experimental slow light results obtained from CPO effects in QWs. In all experiments, a pump laser and a probe laser of frequencies ν_p and ν_s, respectively, are used to create the coherent beating of carriers, which changes the absorption and refractive index spectra seen by the probe laser. In the first experiment [8, 9], a surface-normal geometry is used and low-temperature (10K) measurements of the absorption dip and refractive index change as a function of pump-probe detuning ($\delta = \nu_s - \nu_p$) are obtained for various pump wavelengths and powers. A slowdown factor is inferred from the dispersion curves. In the second experiment [10], surface-normal geometry is also used. Time-domain measurements were made by modulating the pump laser with a single-tone, sinusoidal signal, which creates two side bands onto the pump laser. The two side bands are used as the probe signals with detunings being the modulation frequency $+\delta$ and $-\delta$. The time delay imposed onto the probe beams manifests itself as a time delay of the sinusoidal modulated signal on the pump

laser, which is directly measured relative to the original signal. In the third experiment [11], we used time-domain measurements at room temperature with a waveguide geometry.

The sample used in experiments 1 and 2 consists of 15 GaAs (135Å)/$Al_{0.3}Ga_{0.7}As$(150 Å) QWs grown by molecular beam epitaxy (MBE) and is mounted on a sapphire disk with the substrate removed. The sample is kept at a temperature of 10K. A continuous-wave (CW) Ti-sapphire laser and a tunable diode laser are used to provide the pump and probe beam, respectively. The two beams are focused onto the same spot of the sample. The probe is split into two beams before the sample, traveling through a Mach-Zehnder interferometer (MZI) with the sample in one arm. The absorption spectra are obtained with transmission measurements with and without the pump laser. A homodyne detection scheme is used at the output of the MZI to measure the dispersive characteristics. This setup allows us to measure both the real and imaginary parts of the complex refractive index simultaneously.

Figure 2 shows the experimental data [8, 9] (from the first experiment) of the absorbance spectrum of the probe light, in the presence of a fixed pump light with its energy near the exciton absorption peak from the first experiment [8]. The pump is polarized in the same direction as the probe light. The background absorption decreases, while the coherent spectral hole opens up with increasing pump intensity, showing clear evidence of excitonic coherent population oscillation. Fig. 3(a) shows absorption and dispersion spectra as a function of detuning for pump and probe intensities of 1 and 0.09 kW/cm^2, respectively. The length, L is the total thickness of the 15 QWs (15x13nm = 195nm). The absorption αL is defined by $I_{out} = I_{in}\exp(-\alpha L)$. The spectra were obtained near the heavy-hole (HH) exciton resonance. The absorption spectra feature a sharp dip centered at zero detuning. The depth of the absorption dip increases with increasing pump intensity. The sharp absorption dip arises from CPO induced by the pump and probe. The absorption dip shows a full-width-at-half-maximum (FWHM) bandwidth of 2 GHz (FWHM), which is inversely proportional to the lifetime of the population grating.

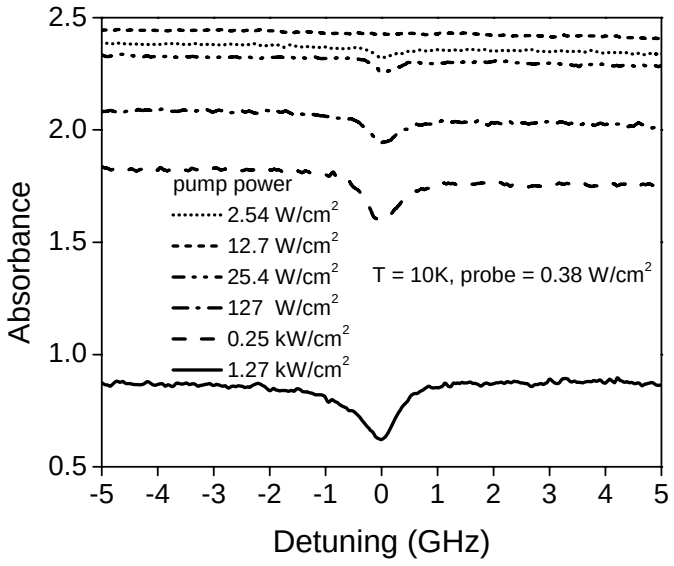

Fig. 2: Experimental results of the absorbance due to excitonic coherent population oscillation in GaAs/AlGaAs QWs at 10K. The zero detuning is set at the pump wavelength which is close to the exciton absorption peak. [8, 9]

The group velocity v_g can be obtained directly from the dispersion of the refractive index. The homodyne signal is proportional to the cosine of the phase delay $\Delta\beta(\nu_s)L$ of the probe beam propagating through the sample. For small variations of the phase delay induced by the pump, the variation of the cosine function can then be approximated by $\Delta\beta(\nu_s)L$. The phase delay of the probe beam is obtained after normalization of the homodyne signal with respect to the absorption spectrum. The slope of the dispersion at zero detuning reveals a slowdown factor of S = 31,200 (Eq. 2), demonstrating a group velocity reduction to 9,600 m/s.

Fig. 3(b) shows the pump intensity dependence of the slowdown factor. The slowdown factor initially increases with increasing pump intensity and peaks before decreasing above 4 kW/cm^2. This behavior is in agreement with the pump intensity dependence of the associated absorption dip, which first shows emergence of the absorption dip, then saturation and broadening as the pump intensity increases.

For a Lorentzian line shape, there is a simple relation between the slowdown factor S at $\delta = 0$, the FWHM bandwidth $\Delta\nu$, and the depth $\Delta\alpha$ of the absorption dip:

$$S = \frac{c}{2\pi}\frac{\Delta\alpha}{\Delta\nu}. \qquad (3)$$

This result arises directly from KK relations and shows how the absorption dip relates to the group velocity reduction. Using Eq. (3), we can calculate the slowdown factor by extracting $\Delta\alpha$ and $\Delta\nu$ from the absorption spectra as shown for the example in Fig. 3(a). The results are plotted in Fig. 3(b) as open circles. As shown in Fig. 3(b), the slowdown factor S obtained from the dispersion measurement agrees well with that obtained from absorption measurement with Eq. (3) though the numerical value from the absorption measurement tends to underestimate the result, possibly due to slight deviations of the absorption dip from an ideal Lorentzian lineshape.

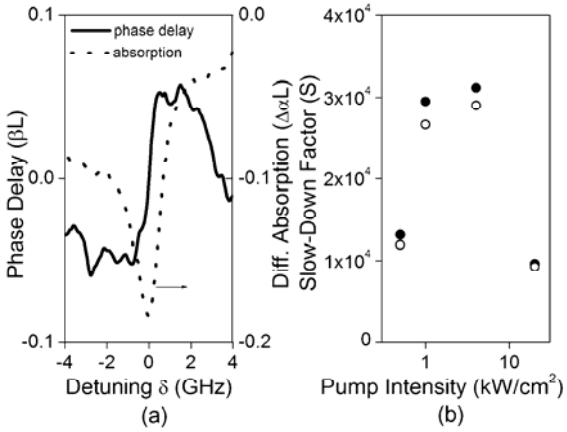

Fig. 3(a) Phase delay (solid line) and absorption (dotted line) experienced by the probe. The slope of the phase delay gives the group velocity. The pump and probe intensities are 1 and 0.09 kW/cm^2, respectively. (b) The pump intensity dependence of the slowdown factor of the group velocity as obtained from dispersion (solid circles) and absorption measurements (open circles). The probe intensity is 6 W/cm^2.

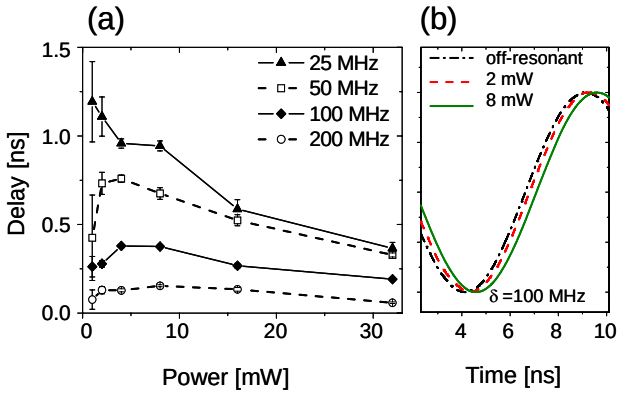

FIG. 4. (a) Power dependence of the time delay at various modulation frequencies. (b) Off-resonant modulation trace and resonant modulation traces at powers of 2 and 8 mW (δ = 100 MHz) demonstrating controllable delay.

2.1.2 Time-Domain Measurements

In the second experiment, time-domain measurements were made with the same 15-QW sample. A RF-amplitude modulation (AM) with a variable frequency *f* is imposed onto a single-mode Ti:Sapphire laser. Sidebands generated by the AM act as the signal, whereas the central band with the carrier wavelength of the laser acts as the pump. The two side bands experience phase change with opposite signs, which thus manifests as a time delay. As pump and signal are effectively imposed onto the same beam, perfect mode matching is guaranteed. The modulation frequency *f* determines the detuning between pump and signal. The sample is cooled to T = 10K and a modulation depth of ~ 5 % is used in the experiment.

At low intensity levels, the width of the CPO absorption dip is determined by the inverse of the HH-exciton lifetime (T_1). The half width at half maximum (HWHM) of 120 MHz corresponds to T_1 = 1.3 ns, which is consistent with previous studies [9]. Note that effects of spatial diffusion are inherently absent in the measurement carried out here as pump and signal fields are co-propagating. This explains the linewidth reduction of the CPO resonance over previous frequency-domain measurements [8].

Fig. 4(a) shows the power dependence of the optical delay for various modulation frequencies. Delays increase at first with increasing power, peak, and roll off as power is further increased. This power dependence reflects the saturation behavior and power broadening of the CPO absorption dip. More importantly, it demonstrates the convenience with which the delay can be tuned optically, as shown in Fig. 4(b). Time delays >1 ns are achieved at *f* = 25 MHz.

Given the length of the active region L (195 nm), this time delay corresponds to group velocities as low as 200 m/s and a slowdown factor $S \sim 1.5\times10^6$.

The greatly increased slowdown factor over that obtained from the first experiment arises mainly from the absence of exciton spatial diffusion [8], which leads to a linewidth/bandwidth reduction and an increase of the transparency depth by a similar factor. The slowdown factor thus shows an overall increase roughly given by the square of the linewidth/bandwidth reduction factor.

In the third experiment, we presented room temperature time-domain measurements of slow-light propagation via CPO on the HH-exciton transition in a (110)-oriented GaAs single quantum well (SQW) waveguide (WG). The WG-geometry provides several advantages over the surface normal geometry. For example, a large and variable optical depth can be easily achieved simply by controlling the length of the WG sample. Due to the strong optical confinement in the WG, the high optical intensities required to achieve CPO at room temperature are more readily attained. Also, carrier diffusion effects are suppressed, as the optical field propagates as a confined WG mode while interacting with the QW region. The use of a waveguide structure also facilitates future device integration. Despite exciton ionization, results are similar to those obtained at low temperature and reflect the general properties associated with a CPO process. More specifically, the measured operating bandwidth is related to the recombination rate of electron-hole pairs. The induced transparency, and hence the maximum achievable fractional delay, scales with the optical depth of the linear response. We demonstrate maximum fractional delays of 3.2% for an initial optical depth of $\Gamma\alpha L \approx 4$, (Γ=confinement factor, α= absorption coefficient, L = sample length).

The quantum well waveguide sample was grown on a (110)-oriented n-type GaAs wafer, including (starting from the substrate) 1.19 μm of $Al_{0.26}Ga_{0.74}As$, 0.17 μm of $Al_{0.15}Ga_{0.85}As$, 60 nm $Al_{0.3}Ga_{0.7}As$, 5.4 nm GaAs QW, 0.345 μm of $Al_{0.3}Ga_{0.7}As$, and a 20 nm GaAs cap layer. The overall structure provides a single-mode planar waveguide. The quantum well is located slightly off center from the fundamental mode. Numerical simulation using this structure shows that only the fundamental mode propagates. The confinement factor Γ is about 1%. The sample was mechanically polished, and a 440-μm long waveguide strip was cleaved. The strip was mounted on a thin copper bridge using silver paste to provide a good thermal contact.

Time-domain measurements were made in a similar manner as in experiment 2. TE-polarized light is coupled in and out of the waveguide. The transmission is characterized carefully as a function of the pump wavelength and detuning/modulation frequency. With L = 440 μm and Γ = 1 %, we obtain $\alpha = 9\times10^3/cm^2$, consistent with typical values of GaAs QW absorption coefficients at room temperature [40-41]. Figure 5(a) shows a generic example of two modulation traces recorded for on- and off-resonant with HH transition, with a modulation frequency f = 100 MHz and input power P = 75 mW. The resonant trace exhibits a delay τ with respect to the off-resonant trace. To demonstrate that the observed slowdown is indeed the effect from CPO, we record a series of modulation traces for different modulation frequencies and input power levels. These results are summarized in Fig. 5(b), in which delay is plotted as a function of modulation frequency at three different power levels. The solid lines are Lorentzian fits centered at f = 0 MHz. Delays up to 830 ps and 3.2 % fractional delay ($\xi = \tau f$) are measured for the highest available input power of P = 75 mW and f = 25 MHz. The inset shows the power dependence of the linewidth (FWHM) $\Delta\nu$, which is obtained from the Lorentzian fits.

For the measured maximum delay of τ = 830 ps, we obtain a slowdown factor S = 565 (using $S = c\tau/L$, L = 440 μm), which is three orders of magnitude smaller than that obtained in our low-temperature study [10]. The discrepancy is mainly due to the fact that we are using a waveguide rather than a surface normal geometry here. Whereas the entire optical mode interacts with the quantum well active region in surface normal geometry, it does so with a significantly reduced confinement factor Γ in the case of a waveguide. The discrepancy in slowdown factors thus mainly reflects the effect of reduced overlap of the optical mode with the active region. A different waveguide design yielding a higher Γ should increase the slowdown factor.

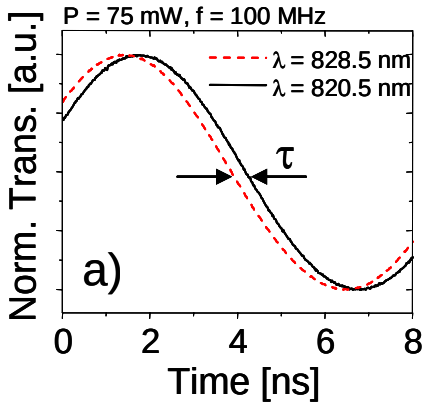

Fig. 5(a) Generic example of two modulation traces recorded on- and off- resonance (f = 100 MHz and P = 75 mW). The trace obtained on-resonance with the HH-excition transition (820.5 nm) is delayed from the reference trace (828.5 nm).

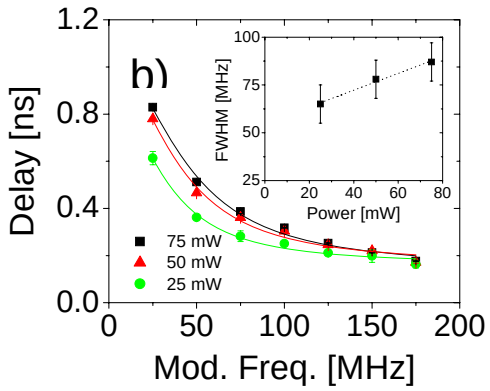

Fig. 5(b) Delay as a function of modulation frequency for P = 25, 50, 75 mW input power. Solid lines are Lorentzian fits. The inset shows the power dependence of the FWHM as obtained from the numerical fits.

2.2 Theory and comparison with experiment [9]

Figure 6 shows a simple two-level system based on the conduction to HH excitonic transition [9, 42]. This two-band model with two spin subsystems can be effectively transformed into two independent two-level subsystems only if the two lowest 1*s* HH excitons of opposite spins are included.

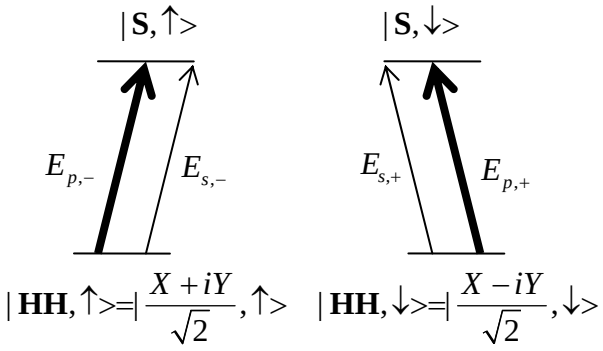

Fig. 6. The level configuration of the excitonic CPO. The positive-helicity components of the pump and signal as well as the spin-down C and HH bands consist of one subsystem while their counterparts form the other.

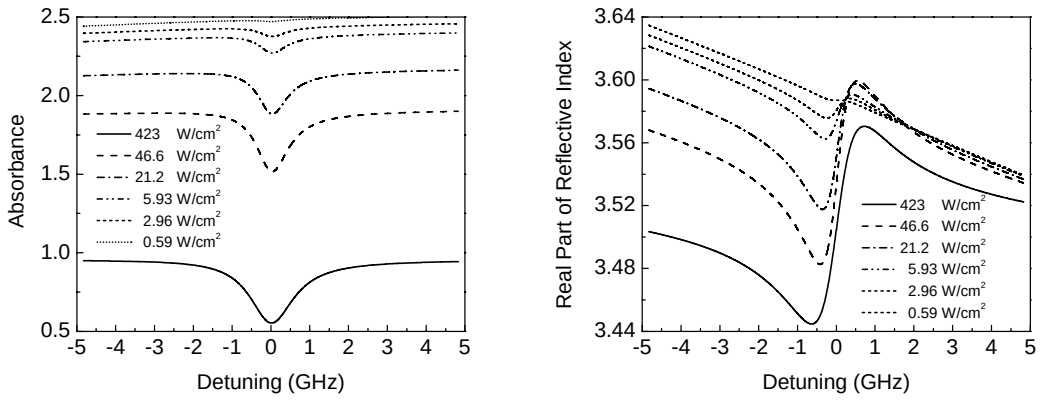

(a) (b)

Fig. 7 (a) The calculated absorbance spectra and (b) the real parts of the refractive index of the optical signal are plotted as a function of the detuning frequency between the signal and pump under different pump intensities. The pump and probe are polarized along the same direction.

We calculate the transmission spectra [9] by taking into account the variation of the refractive index and absorption in the QW region. The theory shows that the absorbance extracted in the experiment [8] can be directly treated as the single-pass absorbance in the QW region. In our theoretical calculations, the excitonic energy $\hbar\omega_{ex}$ is 1.5358 eV, and the photon energy of the pump $\hbar\omega_p$ is the same as the excitonic energy. The sample used in the experiment consists of 15 GaAs/$Al_{0.3}Ga_{0.7}As$ QWs. The barrier width between two QWs is 150 Å. The width of each QW is about 135 Å. The effective length of the absorption region L_{eff} is thus 15×135 Å = 2025 Å.

Figure 7(a) shows the calculated absorbance spectra for the parallel-polarization configuration under different pump intensities. This calculation is performed by matching the background saturated absorption and magnitude of the spectral dip. Other variables in the model include variation of pump intensities, population relaxation constant Γ_1 (=1/T_1), the intrinsic dephasing constant $\Gamma_2^{(0)}$, and a constant γ which describes the excitation induced dephasing. The absorbance spectrum is the product of the absorption spectrum and the effective length of the absorption region. The corresponding real parts of the refractive index are shown in Fig. 7(b). With increased pump intensity, the background absorbance is gradually saturated due to power broadening. When the signal detuning is roughly within the range of the population relaxation constant Γ_1, an absorption dip is created. For direct-gap semiconductors, the bandwidths are about a few gigahertz. The spectral width of the dip is also broadened as the pump intensity is increased. The ratio between the depth and background saturated absorbance increases as the pump intensity gets higher. However, theoretically, the real depth of the dip has a maximum at a particular pump intensity. From the Kramers-Kronig relation, the real part of the refractive index corresponding to the absorption dip must have a rapid increase as the frequency of the signal detuning increases. In Fig. 7(b), the slope of the real part of the refractive index at zero detuning initially increases as the pump intensity gets higher, which reflects the increase of the depth of the spectral dip. However, two factors stop the increase of the slope at high pump intensity. The first one is the broadening of the spectral width of the dip as the pump intensity increases, which widens the window of fast variation of the real part of the refractive index takes place and thus reduces the slope. The second one is the saturated background absorption limiting the absolute depth of the dip. The variation of the real part of the refractive index is subjected to this saturation and results in the decrease of the slope.

Besides the rapid change of refractive index in a local frequency range, the global offset of the refractive index also varies as the pump intensity changes. Theoretically, if the change of dielectric constant caused by the optical transition is small compared with the background dielectric constant, the offset should remain constant as the pump increases. This constant will reflect the background dielectric constant only. On the other hand, if the change of the dielectric constant is significant enough, this offset will be modified by the change of dielectric constant itself. For excitonic CPO, because a large and rapid change is created in a narrow frequency range, there is no guarantee of the constancy of this offset.

A comparison between the theory curves in Fig. 7(a) can be made with the experimental curves in Fig. 2. For details, please refer to Ref. [8, 9]. The pumping intensities for the fitting are set as 0.00059, 0.00298, 0.00593, 0.0212, 0.0466, and 0.423 kW/cm^2. They are chosen to match the background saturated absorbance. The intensities used in theoretical fitting are about one-third or one-fifth of the experimental values. The discrepancy may result from the fact that the

actual pump intensity entering the absorption region is not as large as the estimated intensity outside the sample. Compared with experiment, the theoretical fitting tends to overestimate the depth of the dips. This may be due to the neglect of several factors in our models including the phase-space filling and the reduction of oscillation strength due to electron-hole plasma screening.

Figure 8(a) shows the experimental result of the phase delay of the signal and the corresponding absorbance as a function of detuning for the parallel-polarization configuration of the pump and probe. The phase delay of the optical signal describes the variation of the real part of the refractive index when the pump is present. In the experiment [8], the measurement was carried out by a Mach-Zehnder interferometer. From the measured phase difference, the variation of the real part of the refractive index and the slowdown factor are experimentally obtained. Figure 8(b) shows the theoretical result for the corresponding experiment. The shape and magnitude of the phase delay and absorbance agree well with those obtained from the experiment. Figure 8(c) shows the calculated slowdown factor from our theoretical results. The peak slow-down factor is about 3.13×10^4, which is in excellent agreement with the value of 3.12×10^4 obtained experimentally.

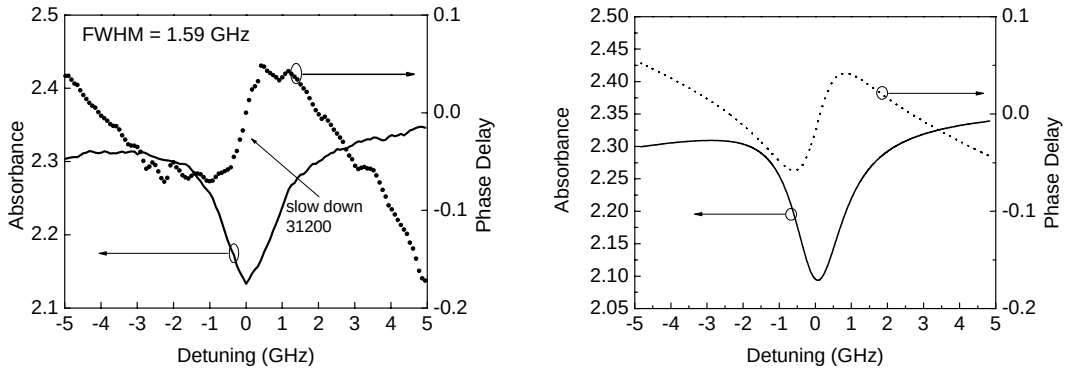

(a) (b)

Fig. 8 (a) Experimental results of the phase delay and absorbance due to excitonic CPO in GaAs/AlGaAs QWs. (b) Our theoretical results agree well with the experimental curves in (a).

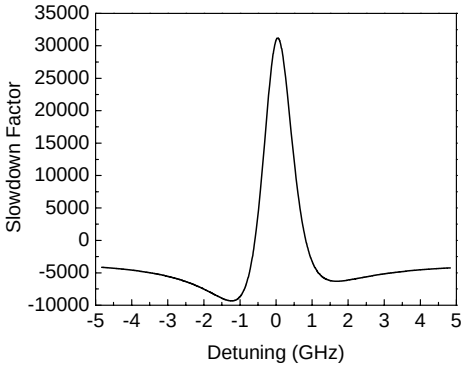

Fig. 8 (c) The theoretical slowdown factor as a function of the detuning frequency between the signal and pump. The peak slowdown factor agrees with the value extracted from the experiment.

3. Slow Light Using EIT in Quantum Wells [1, 21-23]

We started this program by proposing to use the HH1, C1 and C2 in QDs as the transition states for EIT. Theoretical calculations were made and published [1]. However, due to the inhomogeneity of state-of-the-art quantum dot (QD) size, we decided that QDs would not be suitable for the experiment.

We began investigations of a different scheme using quantum wells, using a novel double-V energy configuration to achieve EIT in semiconductors [1,47]. In this scheme, we utilized the C1-LH1 transition. Using the fact that the reported spin coherence lifetime for electrons in (110)-oriented GaAs QWs was quite long [43-45], we explored a configuration using LH1 spin-down (|2>) and C1 spin-up (|3>) as the pump transition, and LH1 spin-down (|2>) and C1 spin-down (|1>) as signal transition. The long coherence time (narrow linewidth) between |3> and |1> provides the necessary condition for EIT. Simultaneously, there exists a degenerate coherent transition between LH1 spin-up (|2'>) and C1 spin-down (|3'>) as the pump transition, and LH1 spin-up (|2'>) and C1 spin-up (|1'>) as the signal. The schematic of the energy configuration is shown in Fig. 9b, which we refer to as the double-V system. In this case, the pump is a TE polarized beam as the summation of two circularly polarized beams for |2>→ |3> and |2'>→ |3'> transitions. The signal beam is a TM polarized beam, identical for both |2>→ |1> and |2'>→ |1'> transitions. This is depicted schematically in Fig. 9 for the case with a magnetic field present, as will be discussed shortly.

In order to realize the system, we used a home-built single-mode Ti:Sapphire ring laser as the pump beam, while the probe is provided by an external cavity tunable diode laser. The two beams collinearly couple into the sample, which is a GaAs(130Å)/$Al_{0.3}Ga_{0.7}As$ single QW slab waveguide, ~150 μm long, grown on an un-doped (110) substrate. We developed the capability to grow GaAs QWs on (110)-oriented substrates using molecular beam epitaxy in a very short amount of time. The very narrow photoluminescence linewidth of ~2 meV at 4 K attests to the excellent quality of the (110) QWs.

EIT based on this double-V energy configuration was subsequently observed for the first time on a (110) QW waveguide. An absorption dip of ~10%, indicating a slow down factor of about 1000, was obtained with a spectral width of ~1 GHz at 4 K. Unlike CPO, where the linewidth of the resonance is determined by the T_1 exciton lifetime, the spectral width in the EIT scheme yields the T_2 dephasing time of the two upper states of the "V" system. Since the upper states of our double-V scheme are the spin-up and spin-down sub-populations of the conduction band, we have in principle a frequency-resolved means of determining the electron spin coherence time in these (110) QW waveguide structures. The result is a coherence time of ~1 ns at 4K, a value similar to other works directly studying (110) GaAs QW spin dephasing [43-45].

In order to unequivocally demonstrate that the observed differential transmission, ~10% transparency, indeed arises from EIT and not CPO, we further designed an in-situ mount to place a permanent magnet inside the cryostat. In a magnetic field, Zeeman splitting of the spin-up and spin-down electrons lifts the conduction band degeneracy, and hence also the degeneracy of the double-V system. Thus for an EIT process, the measurement reveals two peaks corresponding to the two spin populations, with no signal present at zero detuning of the pump and signal beams.

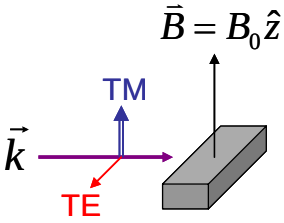

Fig. 9a schematic of magnetic field relative to the QW waveguide. Both probe and pump propagate in direction parallel to QW plane and B field is along 110 direction, normal to substrate.

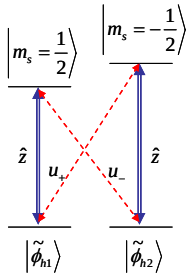

Fig. 9b schematic of energy configuration under the magnetic field, which splits the two spin electronic states.

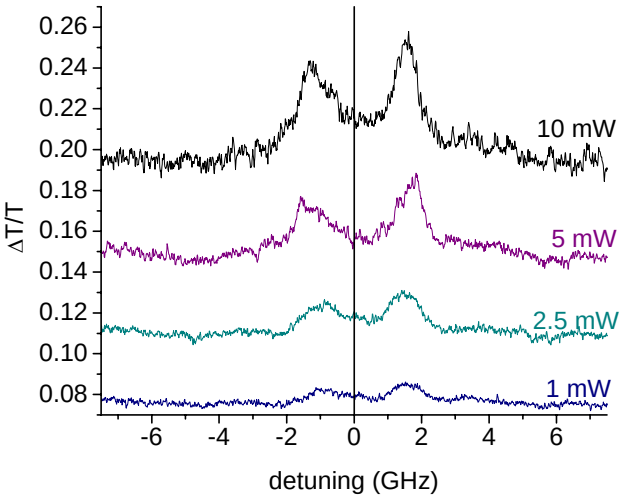

Fig. 10 Differential transmission for 110 QW under magnetic field, showing two distinct EIT peaks corresponding to the energy split due to the magnet.

Conversely, a CPO process would not be affected by the magnetic field, and hence remain as a single peak centered at zero detuning. As shown in Fig. 10, the clearly resolved double-peak structure proves the optical effect observed originates from EIT.

This technique for probing spin coherence is based on Ref. [46], which employs the quasi-monochromatic continuous-wave (CW) pump-probe configuration to optically induce and measure the spin dephasing with (100) GaAs QWs. The present experiments are also in contrast to previous (110) work, which use time-resolved photoluminescence measurements with femtosecond pulses as the excitation source [43-45].

We can systematically characterize the ΔT/T behavior as a function of pump intensity and temperature. Thus far, a maximum ΔT/T of 10.2% was obtained at a 7.6 mW pump power at 40 K on the (110) waveguides, corresponding to a slowdown factor of $S \sim 1000$. Fig. 10 shows ΔT/T traces plotted at various pump powers. With the magnet mounted above the sample in the cryostat, the split in energy is clearly seen.

The magnitude of this peak separation is

$\Delta E_e = \pm g_s \mu_B B$, which follows from Zeeman splitting. Here B is the strength of the magnetic field, nominally 0.3 T, μ_B the Bohr magneton, and g_s the electronic g-factor. By using the unique wavelength resolution afforded by this type of CW measurement, we can also examine how this splitting changes with pump wavelength, polarization, intensity, and temperature. A comparison of these measurements between the (110) and (100) waveguide samples should provide a more complete picture of the EIT process in these QW structures, and is currently under way.

4. Figures of Merit

There has been much interest in developing a set of universal figures of merit (FOM) to compare the trade-off between various schemes to attain slow light – in particular, the delay-bandwidth product (DBP), storage density or device size, and power consumption. We recently analyzed the first two parameters analytically by considering a device with a hole in its absorption spectra [36]. Similar delay-bandwidth analyses are published for CPO and other physical mechanisms [35]. A common conclusion seems to arrive from a number of different authors to lead to a DBP limit of the order of 2. For the absorbers, the maximal delay time will be limited by the residual loss experienced by the signal as well as pulse distortion due to the loss spectra. On the other hand, for SOAs, the maximal delay will be limited by a reasonable SOA gain that can be experienced by the signal (25~30 dB), which is in turn limited by the beating noise of signal and amplified spontaneous emission (ASE). As such, the limitation on the SOA gain limits the number of stored bits to a value between one and two [36].

A yet more relevant question is the trade-off between increased bit rate and storage for a given acceptable power penalty. Here, storage is defined as the number of bits stored, or simply, DBP. We numerically simulated the bit error rate performance for such links [37], showing that storage-bandwidth product (SBP) is an excellent FOM. In the following, we summarize the key findings.

First, the storage density has been shown to be $D = (n_{\max} - n_{\min})/2\lambda_0 = \Delta n / 2\lambda_0$. And for an absorption based device, $D = \Delta\alpha / 4\pi$. This parameter is of critical importance when one is interested in reducing physical size of optical buffers. We also showed the analytical formula for DBP, $TB = L\Delta\alpha / 4\pi$ [36], is established with the bandwidth defined by the change in absorption coefficient. The delay-bandwidth product, *TB*, in this case, is predicted to scale linearly with *L*. However, as shown in [36], for a waveguide device, bandwidth is more appropriately calculated from the transmission through the medium: $T = \exp(-\alpha L)$. We showed that within the range of device lengths that are of interest (1 mm < *L* < 100 mm), the transmission bandwidth is actually proportional to $L^{-1/2}$. Hence, with the delay being proportional to *L*, the delay-bandwidth product (storage) is proportional to $L^{1/2}$. The storage-bandwidth is thus a constant and has no *L* dependence. We further showed that a given system with a given power penalty will have a storage-bandwidth product value which can be used as a FOM.

Power consumption is a critical FOM. However, it is also the most complicated one that depends tremendously on assumptions employed in making the comparisons. It is a subject that is currently under study. However, this issue will remain relatively under explored until the DBP and SBP can be significantly increased in room-temperature operated devices.

5. Conclusions

In conclusion, we have discussed recent progress on slow and fast light using semiconductor QW and QD devices. Significant progress has been made during the last few years under the support of this DARPA program, from very low temperature to room temperature operation. Coherent population oscillation effects have been used in quantum-well and quantum-dot semiconductor optical amplifiers under either forward or reverse biased conditions. Both electrical and optical controls of slow light in frequency as well as time domain measurements have been demonstrated. Challenging issues such as increasing the delay-bandwidth and storage-bandwidth products remain to be solved for future practical applications.

6. References

1. C. J. Chang-Hasnain, P. C. Ku, J. Kim, and S. L. Chuang, “Variable optical buffer using slow light in semiconductor nanostructures,” Proc. IEEE, vol. 9, pp. 1884, 2003.
2. R. S. Tucker, Pei-Cheng Ku, and Constance J. Chang-Hasnain, “Slow-light optical buffers: capabilities and fundamental limitations,” IEEE J. Lightwave Technol., vol. 23, pp. 4046, 2005.
3. G. Lenz, B. J. Eggleton, C. K. Madsen, and R. E. Slusher, “Optical delay lines based on optical filters,” IEEE J. Quantum Electron., vol. 37, no. 4, pp. 525-532, April 2001.
4. A. Yariv, Y. Xu, R. K. Lee, and A. Scherer, "Coupled-resonator optical waveguide: a proposal and analysis," Opt. Lett., vol. 24, pp. 711-713, 1999.
5. P. C. Ku, C. J. Chang-Hasnain, J. Kim, and S. L. Chuang, “Semiconductor all-optical buffers using quantum dots in resonator structures,” Optical Fiber Communications Conference, Atlanta, GA, March 2003.
6. C. Liu, Z. Dutton, Cyrus H. Behroozi, Lene V. Hau, “Observation of coherent optical information storage in an atomic medium using halted light pulses,” Nature, vol. 409, pp. 490-493, 2001.
7. M. S. Bigelow, N. N. Lepeshkin, and R.W. Boyd, “Observation of ultraslow light propagation in a ruby crystal at room temperature,” Phys Rev. Lett., vol. 90, 113903, 2003.
8. P.-C. Ku, F. Sedgwick, C. J. Chang-Hasnain, P. Palinginis, T. Li, H. Wang, S.-W. Chang and S.-L. Chuang, “Slow light in semiconductor quantum wells,” Opt. Lett., vol. 29, pp. 2291-2293, 2004.
9. S. W. Chang, S. L. Chuang, P. C. Ku, C. J. Chang-Hasnain, P. Palinginis, and H. Wang, “Slow light using excitonic population pulsation,” Phys. Rev. B, vol. 70, pp. 235333-1 to 235333-11, 2004.
10. P. Palinginis, S. Crankshaw, F. Sedgwick, E.-T. Kim, M. Moewe, C. J. Chang-Hasnain, H. Wang, and S. L. Chuang, “Ultraslow light (<200 m/s) propagation in a semiconductor nanostructure,” Appl. Phys. Lett., vol. 87 (17), 171102, Oct. 2005.
11. P. Palinginis, F. Sedgwick, S. Crankshaw, M. Moewe, C. J. Chang-Hasnain, “Room temperature slow light in a quantum-well waveguide via coherent population oscillation,” Opt. Express, vol. 13 (24), pp. 9909-9915, November 2005.
12. A. V. Uskov and C. Chang-Hasnain, “Slow and superluminal light in semiconductor optical amplifiers,” Electron. Lett., 41 (16), pp. 55-56, (2005).

13. A. Uskov, Forrest Sedgwick, and Constance J. Chang-Hasnain, “Delay limit of slow light in semiconductor optical amplifiers,” IEEE Photon. Technol. Lett., Vol. 18, 6, pp. 73 –733, March 2006.
14. B. Pesala, Z. Chen, C. Chang-Hasnain, “Tunable pulse delay demonstration using four-wave mixing in semiconductor optical amplifiers”, OSA Topical meeting of Slow and Fast Light, Washington, D. C., 23-26 July, 2006.
15. H. Su and S. L. Chuang, “Variable optical delay using population oscillation and four-wave-mixing in semiconductor optical amplifiers,” Opt. Express, vol. 14, pp. 4800-4807, 2006.
16. H. Su, P. K. Kondratko, and S. L. Chuang, “Electrically and optically controllable optical delay in a quantum-well semiconductor optical amplifier,“ Quantum Electronics and Lasers Sciences, Long Beach, CA, May, 2006.
17. Y. Okawachi, M. S. Bigelow, J. E. Sharping, Z. Zhu, A. Schweinsberg, D. J. Gauthier, R. W. Boyd, and A. L. Gaeta, “Tunable all-optical delays via Brillouin slow light in an optical fiber,” Phys. Rev. Letts., vol. 94, 153902, 2005.
18. A. E. Willner, L. Zhang, T. Luo, C. Yu, W. Zhang and Y. Wang, “Data bit distortion induced by slow light in optical communication systems,” Proc. of SPIE, vol. 6130, 61300T-1, 2006.
19. Y. Okawachi, M. A. Foster, J. E. Sharping, and A. L. Gaeta, Q. Xu and M. Lipson, “All-optical slow-light on a photonic chip,” Opt. Express, vol.14 (6), pp. 2317, 2006.
20. D. Dahan, , G. Eisenstein, “Tunable all optical delay via slow and fast light propagation in a Raman assisted fiber optical parametric amplifier: a route to all optical buffering,“ Opt. Exp. 13, 6234 (2005).
21. P. C. Ku, C. J. Chang-Hasnain, and S. L. Chuang, “Variable semiconductor all-optical buffer,” *Electron. Lett*., vol. 38, pp. 1581-1583, 2002; J. Kim, S. L. Chuang, P. C. Ku, and C. J. Chang-Hasnain, “Slow light using semiconductor quantum dots,” J. Phys.-Cond. Matter, vol. 16, pp. S3727-S3735, 2004.
22. Forrest Sedgwick, Shanna Crankshaw, Michael Moewe, Connie J. Chang-Hasnain, Hailin Wang, Shun-Lien Chuang, “Electron Spin Coherence in (110) GaAs Quantum Well Waveguides,” QELS, Long Beach, CA, 22-26 May 2006.
23. S. L. Chuang, S. W. Chang, and H. Su, “Slow light using semiconductor quantum wells and quantum dots for future optical networks,” International Conference on Solid State Devices and Materials (SSDM), Kobe, Japan, Sept. 12 -15, 2005.
24. S. Sarkar, Y. Guo, and H. Wang, "Tunable optical delay via carrier induced exciton dephasing in semiconductor quantum wells," Opt. Express **14**, 2845-2850 (2006)
25. J. Mørk, R. Kjær, M. van der Poel, L. Oxenløwe, and K. Yvind, “Slow light in a semiconductor waveguide at gigahertz frequencies,“ Opt. Express, 13, pp. 8136-8145, 2005.
26. M. R. Fisher, S.L. Chuang, “Variable group delay and pulse reshaping of high bandwidth optical signals,” IEEE J. Quantum Electron., vol. 41 (6), pp. 885-891, 2005.
27. S. Minin, M. Fisher, and S. L. Chuang, “Current-controlled group delay using a semiconductor Fabry-Perot amplifier,” *Appl. Phys. Lett.*, vol. 84, pp. 3238-3240, 2004.
28. M. R. Fisher, S. Minin, and S. L. Chuang, “Tunable optical group delay in an active waveguide semiconductor resonator,” *IEEE J. Select. Topics Quantum Electron.*, vol. 11, pp. 197-203, 2005.
29. H. Su and S. L. Chuang, “Room temperature slow light with semiconductor quantum-dot devices,” Opt. Lett., vol. 31, pp. 271-273, 2006.
30. H. Su and S. L. Chuang, “Room temperature slow and fast light in quantum dot semiconductor optical amplifiers,” Appl. Phys. Lett., vol. 88, pp. 061102-1 to -3, 2006.

31. P. K. Kondratko, H. Su, and S. L. Chuang, “Room temperature variable slow light using semiconductor quantum dots,“ Conf. Lasers and Electro-Optics (CLEO), Long Beach, CA, May, 2006.
32. P. K. Kondratko, S. W. Chang, H. Su, and S. L. Chuang, “Variable slow light using coherent population oscillation in quantum-dot electroabsorption modulator,“ OSA Topical meeting of Slow and Fast Light, Washington, D. C., 23-26 July, 2006.
33. X. Zhao, P. Palinginis, B. Pesala, C. J. Chang-Hasnain, and P. Hemmer, “Tunable ultraslow light in vertical-cavity surface-emitting laser amplifier,” Optics Express, 13 (20), p. 7899, (2005)
34. X. Zhao, Y. Zhou, C. J. Change-Hasnain, W. Hofmann, M. C. Amann, “Slow and Fast Light Using Master-Modulated Injection-Locked VCSELs,” CLEO, Long Beach, CA, 22-26 May 2006
35. R. W. Boyd, D. J. Gauthier, A. L. Gaeta, and A. E. Willner, "Maximum time delay achievable on propagation through a slow–light medium", Phys. Rev A, vol. 71, 023801, 2005.
36. R. S. Tucker, P.C. Ku, C. J. Chang-Hasnain, “Delay-Bandwidth Product and Storage Density in Slow-Light Optical Buffers,” Electronics Letters, vol. 41, pp. 61, 2005.
37. F. G. Sedgwick, C.J. Chang-Hasnain, P.C. Ku, and R.S. Tucker, “Storage-bit-rate product in slow-light optical buffers,” Electronics Letters, vol. 41 (24), pp. 1347-1348, November 2005
38. J. B. Khurgin, “Optical buffers based on slow light in electromagnetically induced transparent media and coupled resonator structures: comparative analysis,” J. Opt. Soc. Am. B, vol. 22, pp. 1062-73, 2005.
39. H. Wang, M. Jiang, and D. G. Steel, “Measurement of phonon-assisted migration of localized excitons in GaAs/AlGaAs multiple-quantum-well structures,” Phys. Rev. Lett., vol. 65, pp. 1255, 1990.
40. D. S. Chemla, D. A. B. Miller, “Room-temperature excitonic nonlinear-optical effects in semiconductor quantum-well structures,” J. Opt. Soc. Am. B, vol. 2, p. 1155, 1985.
41. H. Haug and S. W. Koch, Quantum Theory of the Optical and Electronic Properties of Semiconductors 3rd ed. (World Scientific, Singapore, 1994).
42. D. Derickson, Fiber Optics Test and Measurement, Chap. 12, (Prentice-Hall, Inc., 1998.)
43. T. Adachi, Y. Ohno, F. Matsukura, H. Ohno, “Spin relaxation in n-modulation doped GaAs/AlGaAs (110) quantum wells,” Physica E **10**, 36 (2001).
44. S. Dohrmann, D. Hagele, J. Rudolph, M. Bichler, D. Schuh, M. Oestreich, “Anomalous Spin Dephasing in (110) GaAs Quantum Wells: Anisotropy and Intersubband Effects,” Phys. Rev. Lett. **93**, 147405 (2004).
45. Y. Ohno, R. Terauchi, T. Adachi, F. Matsukura, and H. Ohno, “Spin Relaxation in GaAs(110) Quantum Wells,” Phys. Rev. Lett **83**, 4196 (1999).
46. S. Sarkar, P. Palinginis, P.C. Ku, C. J. Chang-Hasnain, N. H. Kwong, R. Binder, H. Wang, “Inducing electron spin coherence in GaAs quantum well waveguides: Spin coherence without spin precession,” Phys. Rev. B **72**, 035343 (2005).
47. S.-W. Chang, S. L. Chuang, C. Chang-Hasnain, and H. Wang, "Slow light using electromagnetically induced transparency in [110] strained quantum wells," American Physical Society, March Meeting, Los Angeles CA, (2005).

Appendix: Researchers and Publications Supported by this Program

Post-docs: Pei-Cheng Ku, Phedon Palinginis, and Eui-tae Kim
Pei-Cheng Ku, PhD Thesis: "Semiconductor Slow-Light Devices", November 2003
Forrest Sedgwick, PhD Thesis, expected August 2007
Other Students: Shanna Crankshaw and Michael Moewe
Shu-Wei Chang, Ph.D. thesis: "Slow Light Based on Quantum Effects in Quantum Wells and Quantum Dots," University of Illinois at Urbana-Champaign, Dept. of ECE, 2006. (Advisor, Professor S. L. Chuang).

1. (Invited) C. J. Chang-Hasnain and S.L. Chuang, "Slow and Fast Light in Semiconductor Quantum-well and Quantum-dot Devices", IEEE Journal of Lightwave Communications, Special Issue on Optoelectronics, Jan. 2007.
2. (Invited) P.C. Ku, C. J. Chang-Hasnain and S.L. Chuang, "Slow light in semiconductor heterostructures", J. Phys. D, Jan. 2007.
3. (Invited) C. J. Chang-Hasnain, P.C. Ku, J. Kim, S.L. Chuang, " Variable Optical Buffer Using Slow Light in Semiconductor Nanostructures," Proceedings of the IEEE, Special Issue on Nanoelectronics and Nanoscale Processing 91 (11), pp. 1884-97, Nov. 2003.
4. Forrest Sedgwick, Shanna Crankshaw, Michael Moewe, Connie J. Chang-Hasnain, Hailin Wang, and Shun-Lien Chuang, "Electron Spin Coherence in (110) GaAs Quantum Well Waveguides", manuscript under preparation.
5. Rodney S. Tucker, Pei-Cheng Ku, and Constance J. Chang-Hasnain, "Slow-Light Optical Buffers: Capabilities and Fundamental Limitations", IEEE Journal of Lightwave Communications 23 (12), pp. 4046 – 4066, Dec. 2005.
6. F.G. Sedgwick, C.J. Chang-Hasnain, P.C. Ku, and R.S. Tucker, "Bit-Rate-Storage Product in Slow-Light Optical Buffers," Electronics Letters 41 (24), pp. 1347-1348, Nov. 2005.
7. Phedon Palinginis, Forrest Sedgwick, Shanna Crankshaw, Michael Moewe, Connie J. Chang-Hasnain, "Room Temperature Slow Light in a Quantum-Well Waveguide via Coherent Population Oscillation," Optics Express 13 (24), pp. 9909-9915, Nov. 2005.
8. Phedon Palinginis, Shanna Crankshaw, Forrest Sedgwick, Eui-Tae Kim, Michael Moewe, Connie J. Chang-Hasnain, Hailin Wang, and Shun-Lien Chuang, "Ultraslow Light (<200 m/s) Propagation in a Semiconductor Nanostructure," Applied Physics Letters 87 (17), 171102, Oct. 2005
9. Xiaoxue Zhao, Phedon Palinginis, Bala Pesala, Connie J. Chang-Hasnain, Philip Hemmer, "Tunable Ultraslow Light in 1550 nm VCSEL Amplifier", Optics Express 13 (20), pp. 7899-7904, Oct. 2005.
10. Rodney S. Tucker, Pei-Cheng Ku, and Constance J. Chang-Hasnain, "Delay-Bandwidth Product and Storage Density in Slow-Light Optical Buffers", Electronics Letters 41 (4), pp. 208-209, Feb. 2005.

11. Pei-Cheng Ku, Phedon Palinginis, Tao Li, Forrest Sedgwick, Shu-Wei Chang, Hailin Wang, Connie J. Chang-Hasnain, and Shun-Lien Chuang, “Slow-light in semiconductor quantum wells”, Optics Letters 29 (19), pp. 2291-2293, Oct. 2004.
12. Shu-Wei Chang, Shun-Lien Chuang, Pei-Cheng Ku, Connie J. Chang-Hasnain, Phedon Palinginis, and Hailin Wang,” Slow light using excitonic population pulsation,” Phys. Rev. B 70, 235333 (2004).
13. J Kim, S L Chuang, P C Ku and C J Chang-Hasnain, “Slow light using semiconductor quantum dots”, J. Phys.-Cond. Matt. 16 (35), pp. S3727-S3735, Sept. 2004.
14. P. C. Ku, C. J. Chang-Hasnain, and S. L. Chuang, “A proposal of variable semiconductor all-optical buffer,” Electronics Letters 38 (24), pp.1581-1583, Nov. 2002.
15. S. Sarkar, P. Palinginis, P.C. Ku, C.J. Chang-Hasnain, N.H. Kwong, R. Binder, H. Wang, “Inducing electron spin coherence in GaAs quantum well waveguides: Spin coherence without spin precession”, Phys. Rev. B 72, 35343 (2005).
16. H. Su, P. Kondratko, S. L. Chuang, “Variable optical delay using population oscillation and four-wave-mixing in semiconductor optical amplifiers,” Optics Express 14 (11) pp. 4800-4807
17. A. V. Uskov, F. G. Sedgwick, C. J. Chang-Hasnain, “Delay limit of slow light in semiconductor optical amplifiers,” IEEE Photonics Technology Letters 18 (5-8) pp. 731-733, Mar.-Apr. 2006
18. H. Su, S. L. Chuang, “Room temperature slow and fast light in quantum-dot semiconductor optical amplifiers,” Applied Physics Letters 88 (6), 061102, Feb. 2006
19. H. Su, S. L. Chuang, “Room-temperature slow light with semiconductor quantum-dot devices,” Optics Letters 31 (2), pp. 271-273 Jan. 2006
20. S. W. Chang, S. L. Chuang, “Slow light based on population oscillation in quantum dots with inhomogeneous broadening,” Phys. Rev. B 72 (23), 235330 Dec. 2005
21. R. S. Tucker, P. C. Ku, C. J. Chang-Hasnain, “Slow-light optical buffers: Capabilities and fundamental limitations,” Journal Of Lightwave Technology 23 (12), pp. 4046-4066 Dec. 2005
22. A. V. Uskov, C. J. Chang-Hasnain, “Slow and superluminal light in semiconductor optical amplifiers,” Electronics Letters 41 (16), pp. 922-924 Aug. 2005
23. S. W. Chang, S. L. Chuang, “Strain-induced enhancement of spin relaxation times in [110] and [111] grown quantum wells,” Phys. Rev. B 72 (11), 115429 Sep. 2005
24. S. Sarkar, Y. Guo, H. L. Wang, “Tunable optical delay via carrier induced exciton dephasing in semiconductor quantum wells,” Optics Express 14 (7), pp. 2845-2850 Apr. 2006
25. S. W. Chang, S. L. Chuang, C. J. Chang-Hasnain, and H. Wang, “Slow light using coherence and V-type EIT in [110] strained quantum wells,” J. Opt. Soc. Am. B, accepted (in press).
26. Forrest Sedgwick, Shanna Crankshaw, Michael Moewe, Connie J. Chang-Hasnain, Hailin Wang, Shun-Lien Chuang, “Electron Spin Coherence in (110) GaAs Quantum Well Waveguides,” QELS, Long Beach, CA, 22-26 May 2006

27. Xiaoxue Zhao, Phedon Palinginis, Bala Pesala, Connie J. Chang-Hasnain, Philip Hemmer, "Tunable Ultraslow Light in 1550 nm VCSEL Amplifier", ECOC postdeadline paper, Glasgow, UK October 2005.
28. Phedon Palinginis, Forrest Sedgwick, Shanna Crankshaw, Eui-tae Kim, Michael Moewe, Connie J. Chang-Hasnain, Hailin Wang, and Shun-Lien Chuang, "Ultra Slow Light (< 200 m/s) Propagation in a Semiconductor Nanostructure", CLEO postdeadline paper, May 2005.
29. Susanta K. Sarkar, Phedon Palinginis, Hailin Wang, Pei-Cheng Ku, Connie J. Chang-Hasnain, N. H. Kwong and R. Binder, "Inducing electron spin coherence in GaAs quantum well waveguides: Spin Coherence without spin precession" QELS May 2005.
30. Susanta Sarkar, Phedon Palinginis, and Hailin Wang, Pei-Cheng Ku and Connie J. Chang-Hasnain, N.H. Kwong and R. Binder, "Inducing electron spin coherence without magnetic fields in GaAs quantum well waveguides", APS Annual Meeting March 2005.
31. Shu-Wei Chang, Shun-Lien Chuang, Connie J. Chang-Hasnain, Hailin Wang, "Slow Light Using Electromagnetically Induced Transparency from Spin Coherence in [110] Strained Quantum Wells", APS Annual Meeting, March 2005.
32. Pei-Cheng Ku, and Constance J. Chang-Hasnain, Rodney S. Tucker, "Link Performance of All-Optical Buffers Using Slow Light", Optical Fiber Communications Conference Technical Digest. Anaheim, CA, 6-11 March, 2005.
33. Rodney S. Tucker, Pei-Cheng Ku, and Constance J. Chang-Hasnain, "Fundamental Limitations of Slow-Light Optical Buffers", Optical Fiber Communications Conference Technical Digest. Anaheim, CA, 6-11 March, 2005.
34. P.C. Ku, L. Chrostowski, C. J. Chang-Hasnain, "A Novel, Low $V\pi$ EIT Based Optical Modulators", IEEE International Topical Meeting on Microwave Photonics. Ogunquit, ME, October 2004.
35. Shu-Wei Chang and Shun-Lien Chuang, Pei-Cheng Ku and Connie J. Chang-Hasnain, Phedon Palinginis and Hailin Wang, "Polarization-Dependent Excitonic Population Pulsation and Slow Light due to Excitation-Induced Dephasing", CLEO, San Francisco, CA, May 2004
36. P. C. Ku, C. J. Chang-Hasnain, J. Kim, and S. L. Chuang, "Slow-Light in Nonuniform Quantum Dot Waveguide", LEOS Annual Meeting, Tucson, AZ, Nov. 2003
37. P. C. Ku, C. J. Chang-Hasnain, J. Kim, and S. L. Chuang, "Novel Semiconductor Mach-Zehnder Modulators with Low Drive Voltage $V\pi$", OSA Annual Meeting, Tucson, AZ, Oct. 2003
38. P. C. Ku, C. J. Chang-Hasnain, J. Kim, and S. L. Chuang, "Semiconductor all-optical buffers using quantum dots in resonator structures," Optical Fiber Communications Conference, Atlanta, GA, March 2003.